

Immunity, Volume 32

## **Supplemental Information**

### **Dependence of T Cell Antigen Recognition**

### **on T Cell Receptor-Peptide MHC Confinement Time**

**Milos Aleksic\*, Omer Dushek\*, Hao Zhang, Eugene Shenderov, Ji-Li Chen, Vincenzo Cerundolo, Daniel Coombs, and P. Anton van der Merwe**

\*These authors contributed equally

## Supplemental Experimental Procedures

### Surface plasmon resonance (SPR)

Binding of 1G4 TCR to pMHC variants was analysed by SPR on a BIAcore 3000 (GE Healthcare). Unless otherwise stated all experiments were performed at 37°C and using a flow rate of 10  $\mu$ l/minute in HBS-EP buffer (0.01 M HEPES buffer (pH 7.4), 0.15 M NaCl, 0.005% Surfactant P20). Biotinylated pMHC was immobilized to CM5 sensor chip (GE Healthcare) indirectly by covalently coupled streptavidin at various levels (250 RU for kinetics and 1000 RU for affinity measuring). To determine affinity of the 1G4 TCR for its ligands, equilibrium binding was measured for graded concentrations of TCR. The  $K_D$  value was obtained by non-linear curve fitting using Origin (OriginLab) to the Langmuir binding isotherm,

$$\text{bound} = C^A * \text{Max} / (C^A + K_D),$$

where “bound” is the equilibrium binding in RUs at injected TCR concentration  $C^A$  and Max is the maximum binding (RUs).

Kinetics of TCR/pMHC interaction was measured by injecting TCR at a flow rate of 50  $\mu$ l/minute over low levels of immobilized pMHC (250 RU) to minimize mass transport effects. Dissociation rate constant  $k_{\text{off}}$  was determined by curve fitting to the 1:1 Langmuir binding model using BIAevaluation (BIAcore software). Association rate constant  $k_{\text{on}}$  was calculated using  $k_{\text{on}}=k_{\text{off}}/K_D$ .

Equilibrium thermodynamics at 25°C were analyzed by measuring  $K_D$  values over a range of temperatures (from 4°C to 37°C), calculating  $\Delta G$  ( $\Delta G=-RT \ln(K_D)$ ), and fitting the nonlinear form of the van't Hoff equation to this data,

$$\Delta G^\circ = \Delta H_{T_o} - T\Delta S_{T_o} + \Delta C_p(T - T_o) - T\Delta C_p \ln(T/T_o),$$

where R is the gas constant ( $R=1.987 \times 10^{-3}$  kcal/(mol K)), T is the temperature in Kelvin (K),  $T_o$  is an arbitrary reference temperature (298.15 K),  $\Delta G^\circ$  is the standard free energy of binding at T (kcal mol<sup>-1</sup>),  $\Delta H_{T_o}$  is the enthalpy change upon binding at  $T_o$  (kcal mol<sup>-1</sup>),  $\Delta S_{T_o}$  is the standard state entropy change upon binding at  $T_o$  (kcal mol<sup>-1</sup> K<sup>-1</sup>), and  $\Delta C_p$  is the change in heat capacity (kcal mol<sup>-1</sup> K<sup>-1</sup>), assumed to be temperature independent.

Thermodynamic parameters for interaction at 37°C were calculated as follows;

$$\Delta G_{37^\circ\text{C}} = -RT \ln(K_D) (37^\circ\text{C}),$$

$$\Delta H_{37^\circ\text{C}} = \Delta H_{25^\circ\text{C}} + 12 * \Delta C_p, \text{ and}$$

$$T\Delta S_{37^\circ\text{C}} = T\Delta S_{25^\circ\text{C}} + 310.15 \text{ }^\circ\text{K} \times \Delta C_p(\ln(310.15^\circ\text{K}/298.15^\circ\text{K})).$$

Transition state thermodynamics were analyzed by measuring temperature dependence of kinetic parameters.  $k_{\text{off}}$  was measured at temperatures ranging from 4°C to 37°C and activation energy of dissociation ( $\Delta^\ddagger G_{\text{diss}}$ ) was calculated using  $\Delta^\ddagger G_{\text{diss}} = -RT \ln(k_{\text{off}}h/k_B T)$ , where h is Planck constant ( $h=6.63 \times 10^{-34}$  J S) and  $k_B$  is Boltzmann constant ( $k_B=1.381 \times 10^{-23}$  J/K). The nonlinear form of the van't Hoff equation was fitted to the data to obtain values for activation enthalpy ( $\Delta^\ddagger H_{\text{diss}}$ ), entropy ( $\Delta^\ddagger S_{\text{diss}}$ ), and heat capacity change ( $\Delta^\ddagger C_{p_{\text{diss}}}$ ) of dissociation. Thermodynamic parameters for association phase were calculated from  $\Delta^\ddagger X_{\text{ass}} = \Delta X + \Delta^\ddagger X_{\text{diss}}$ , where X represents  $\Delta G$ ,  $\Delta H$ ,  $\Delta S$ , or  $\Delta C$ .

## TCR and pMHC production

NY-ESO-1<sub>156–157</sub> APLs were synthesized by standard solid-phase chemistry on a multiple peptide synthesizer (Genosys) using F-moc for transient NH<sub>2</sub>-terminal protection. All peptides were > 90% pure, as indicated by analytical HPLC. HLA-A2 heavy chain (residues 1-278) with C-terminal BirA tag and  $\beta_2$ -microglobulin were expressed as inclusion bodies in E.coli, refolded in vitro in the presence of synthesized NY-ESO-1<sub>156–157</sub> APLs, and purified using size-exclusion chromatography [1]. Purified pMHC was biotinylated in vitro by BirA enzyme (Avidity). Modified HLA-A2 was generated by replacing amino-acids that lie at a distance shorter than 6 angstroms from the 1G4 TCR, using information from the crystal structure of 1G4 TCR in complex with ESO-9C/HLA-A2 [2]. Amino-acid substitutions were introduced in HLA-A2 expressing plasmid using a QuickChange site directed mutagenesis kit (Stratagene). Modified HLA-A2 proteins were all refolded with the ESO-9V peptide since this peptide has been shown to have improved affinity for MHC [2]. The 1G4 TCR subunits,  $\alpha$  and  $\beta$ , were expressed in E.coli as inclusion bodies, refolded in vitro, and purified using size exclusion chromatography (as described in [3]).

## T-cell stimulation by plate-bound pMHC

To obtain various levels of pMHC surface immobilization, serial dilutions of each pMHC (100  $\mu$ g/ml - 300 pg/ml) were incubated in wells of SigmaScreen streptavidin coated 96-well plates (Sigma) for 90 minutes at 4°C. Two plates were prepared, the first used for the stimulation assay and the second was used to determine the levels of correctly folded plate-immobilized pMHC. For the cell stimulation assay, 5000 1G4 CTLs were incubated in pMHC coated plates for 4h at 37°C and the concentration of released IFN- $\gamma$  in the supernatants was measured by ELISA using the OptEIA Human IFN- $\gamma$  ELISA set (BD Biosciences). EC<sub>50</sub> values for each ligand were obtained by fitting a sigmoid dose-response model to the data using Origin (OriginLab Corporation). Levels of active plate-immobilized pMHC were measured on the second plate by ELISA using the W6/32 mouse anti human MHC class I antibody specific for correctly folded pMHC in combination with HRP conjugated donkey anti-mouse IgG antibody (Jackson Immunoresearch). Measured EC<sub>50</sub> values for IFN- $\gamma$  secretion were then corrected by a factor representing fold difference in pMHC immobilization levels compared to ESO-9V/A2, which was chosen as a reference pMHC.

## Cytotoxicity assay

We used a Transporter Associated with Antigen Processing (TAP) deficient T2 cell line pulsed with ESO-9V APLs as target cells. As a consequence of a defect in antigen processing, the T2 cell line expresses low levels of short-lived pMHC [4] and the addition of exogenous peptides significantly increases pMHC surface expression [4]. Since the effect of exogenous peptides on MHC stabilization in T2 cells can be variable, we first analyzed the effect ESO-9V APLs have on the increase in HLA-A2 levels in T2 cells. 100 000 T2 cells were incubated with various concentrations of peptides for 3 hours, stained with 10  $\mu$ l/ml FITC labeled anti-HLA-A2 antibody (BB7.2 clone, BD), and HLA-A2 expression levels were analyzed by FACS (Figure S2D). The peptide concentration yielding a 40% increase of correctly folded surface HLA-A2 (C<sub>40%</sub>) was determined for each peptide. Target cells were prepared by labeling 5000 T2-cells with <sup>51</sup>Cr (50  $\mu$ Ci/million cells) for 90 minutes at 37°C, washing, and incubating for 1h at 37°C with serial dilution of specific peptides, starting from determined C<sub>40%</sub> concentration. The cytotoxicity assay was then performed

by adding 5000 1G4 CTLs to target cells for 4h at 37°C. Levels of released  $^{51}\text{Cr}$  from lysed cells were measured using a Microbeta counter (PerkinElmer). The percent of specific lysis was calculated from  $100 \times ((\text{experimental release} - \text{spontaneous release}) / (\text{maximal release} - \text{spontaneous release}))$ . Maximal  $^{51}\text{Cr}$  release was measured by lysing target cells in 5% Triton X-100 and spontaneous release was found by measuring  $^{51}\text{Cr}$  release from control target cells that were incubated without peptides.

### Correlating the T cell response to TCR-pMHC bond parameters

As in previous studies, we have used the concentration of pMHC required to induce half-maximal response ( $\text{EC}_{50}$ ) as an indicator of pMHC potency and in what follows pMHC potency is the dependent variable,  $y$ . The parameters governing the TCR-pMHC bond (e.g.  $K_D$ ,  $k_{\text{off}}$ ,  $k_{\text{on}}$ ,  $\Delta C_p$ , etc) are the independent variables which we define as  $x$ . We begin by assuming a simple linear relationship between pMHC potency and the parameters governing the TCR-pMHC bond,

$$y = b_0 + b_1x$$

where  $b_0$  and  $b_1$  are model parameters. All data fitting is performed using the Matlab function `lsqcurvefit`. Using the sum of squared residuals (SSR) we compute the  $R^2$  statistic, which is the square of the correlation coefficient in this simple linear model. Using standard methods we obtain a p-value for the null hypothesis that the parameter  $b_1 = 0$  (i.e. small p-values indicate the model is significant). Briefly, p-values are computed by calculating an F-score that accounts for the number of data points and the number of fitted parameters (2 in this case). Table 1 in the main text summarizes this analysis. Significant correlations ( $p < 0.05$ ) are obtained only with  $K_D$ ,  $k_{\text{off}}$ , and  $k_{\text{on}}$ . Significant correlations are observed with other quantities (e.g.  $t_{1/2}$ ,  $\Delta G$ , etc) as they are derived from either  $K_D$  or  $k_{\text{off}}$ .

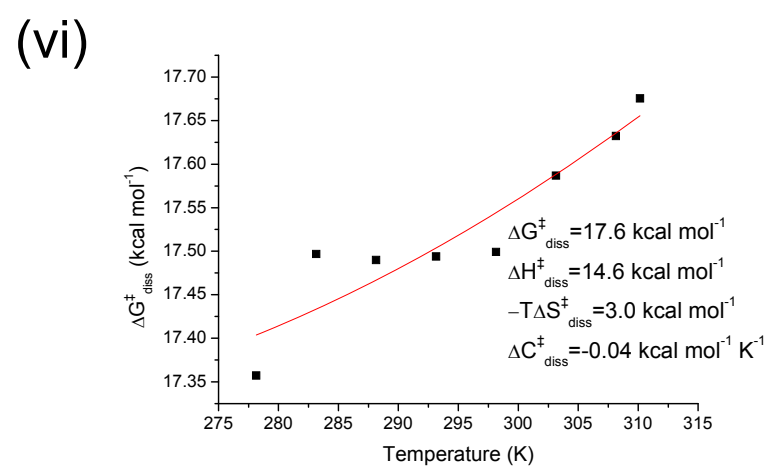
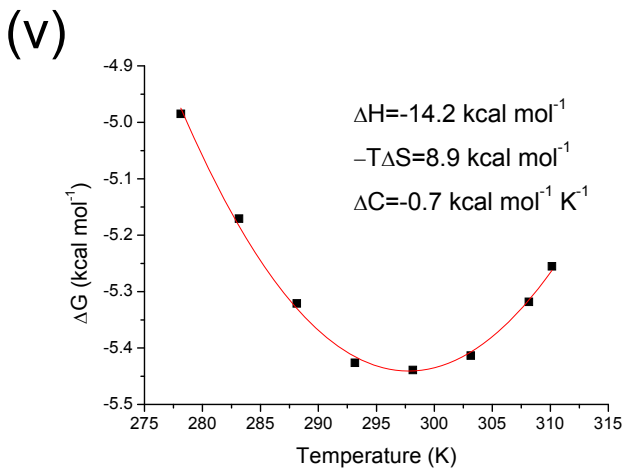
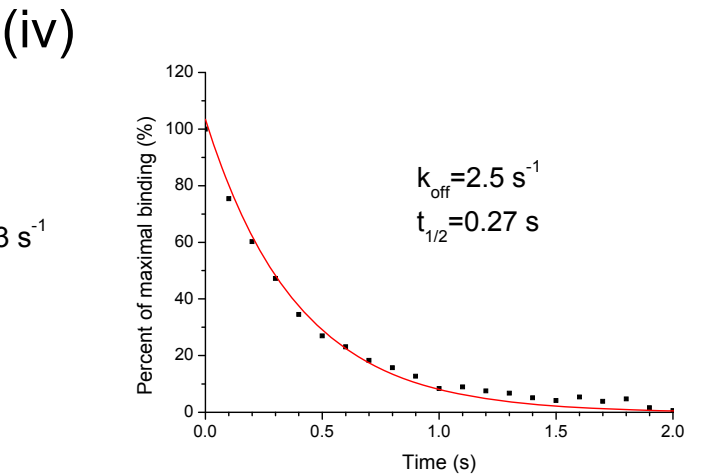
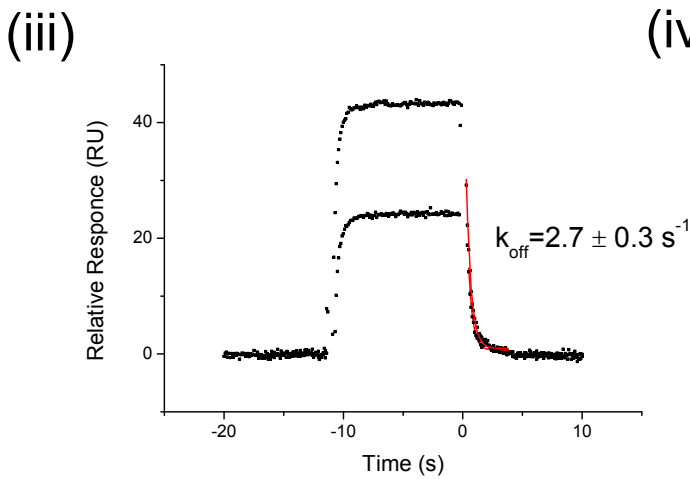
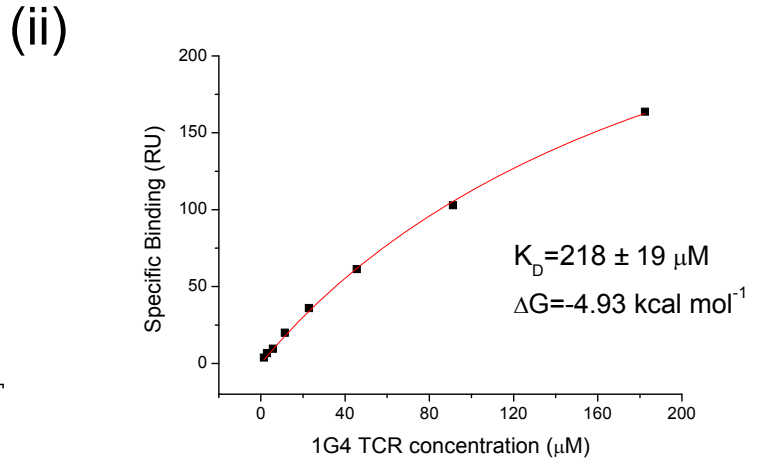
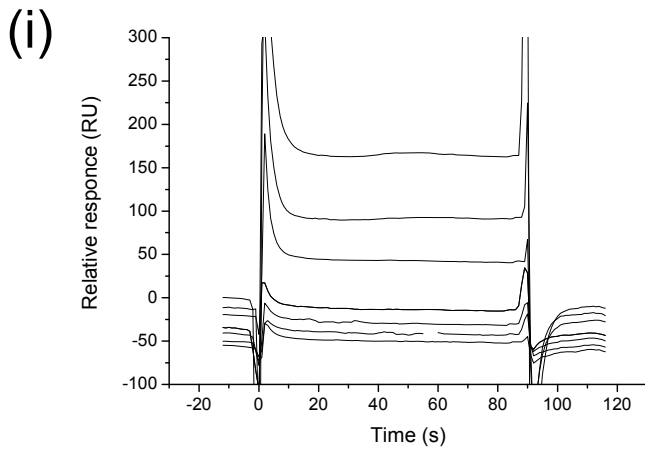
As described above, the measure of pMHC potency ( $y$ ) is the concentration required to elicit half-maximal IFN- $\gamma$  secretion ( $\text{EC}_{50}$ ). We have introduced error into the analysis by using  $\text{EC}_{50}$  directly, instead of  $\log_{10}(\text{EC}_{50})$  (which is obtained from data fitting), because we expect TCR-pMHC bond parameters to be directly correlated to  $\text{EC}_{50}$ . The introduced error is expected to be small because  $\text{EC}_{50}$  values span less than an order of magnitude. We have also fit the data for  $\text{EC}_{50}$  directly (instead of  $\log_{10}(\text{EC}_{50})$ ) and obtained similar values. Repeating all the calculations we find quantitative differences (e.g. lower  $R^2$  values for all models) but conclusions are unchanged (not shown).

In a second assay of pMHC potency, a measure of cytotoxicity is implemented. In this assay the agonist pMHC is diluted by null pMHC and therefore we expect that the relevant correlate will be  $1/\text{EC}_{50}$ . However, we found that the residuals from data fits were not randomly distributed (Figure S3A) and the log-transform provided randomly distributed residuals (Figure S3B). We speculate that there may be a non-linear relationship between the concentration of incubated peptide and the level of pMHC presented to T cells by APCs. We have therefore taken the measure of pMHC potency to be  $y = 1/\log_{10}(\text{EC}_{50})$ , which provides the largest  $R^2$  values. We find quantitative differences when  $y = 1/\text{EC}_{50}$  is used (mainly lower  $R^2$  values) but conclusions are unchanged (not shown).

## References

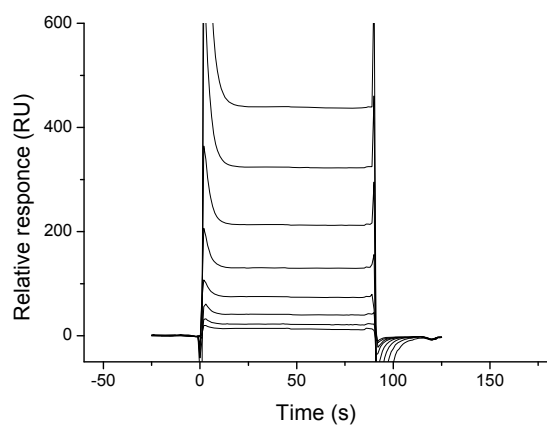
1. Madden DR, Garboczi DN, Wiley DC (1993) The antigenic identity of peptide-MHC complexes: a comparison of the conformations of five viral peptides presented by HLA-A2. *Cell* 75:693–708.
2. Chen JL, Stewart-Jones G, Bossi G, Lissin NM, Wooldridge L, et al. (2005) Structural and kinetic basis for heightened immunogenicity of T cell vaccines. *J Exp Med* 201:1243–1255.
3. Boulter JM, Glick M, Todorov PT, Baston E, Sami M, et al. (2003) Stable, soluble T-cell receptor molecules for crystallization and therapeutics. *Protein Eng* 16:707–711.
4. Cerundolo V, Alexander J, Anderson K, Lamb C, Cresswell P, et al. (1990) Presentation of viral antigen controlled by a gene in the major histocompatibility complex. *Nature* 345:449–452.

# a) ESO-4D

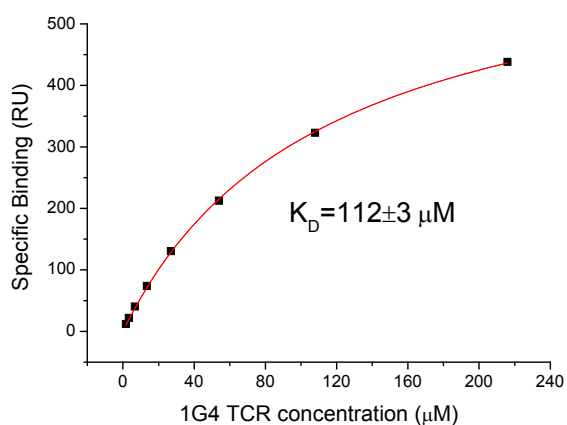


## b) ESO-R65

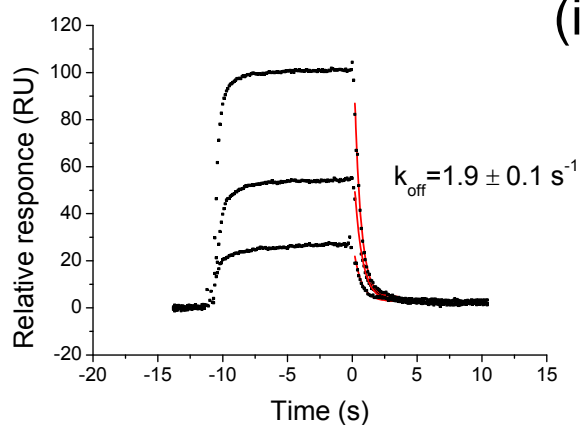
(i)



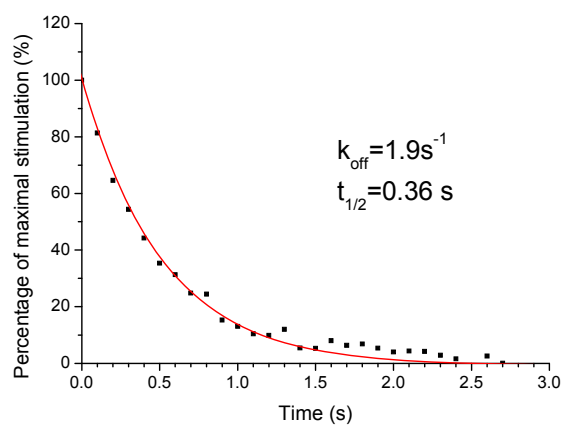
(ii)



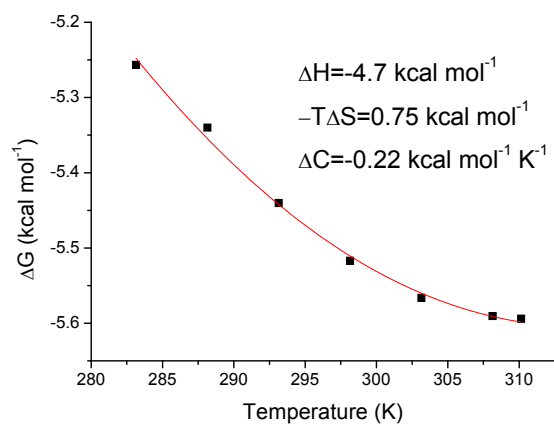
(iii)



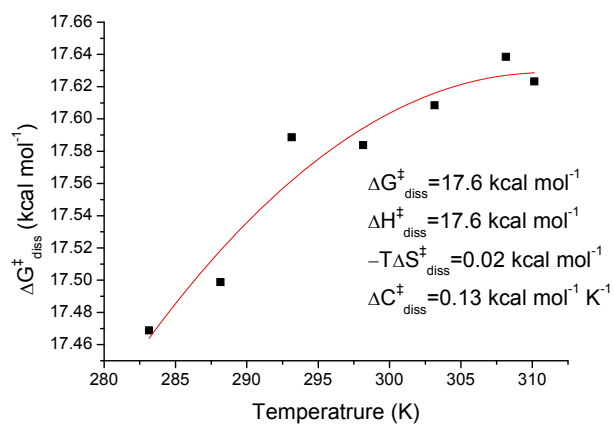
(iv)



(v)

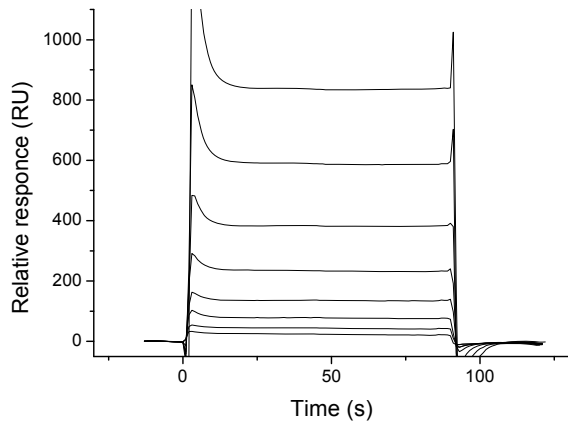


(vi)

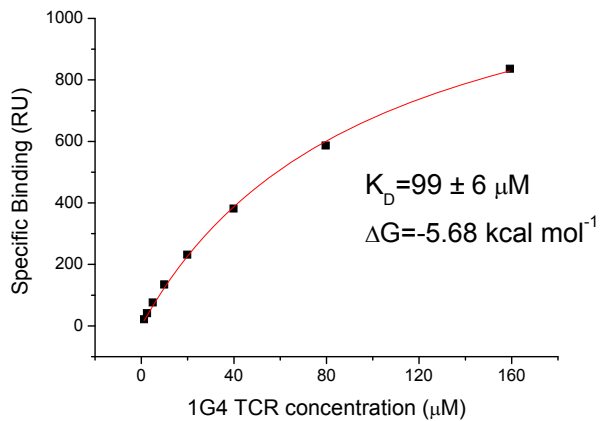


# c) ESO-6T

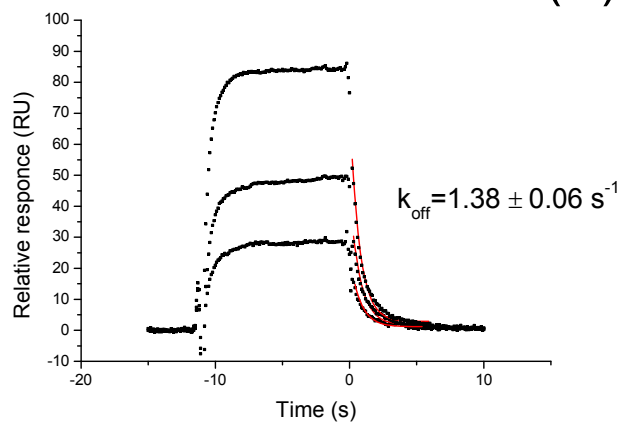
(i)



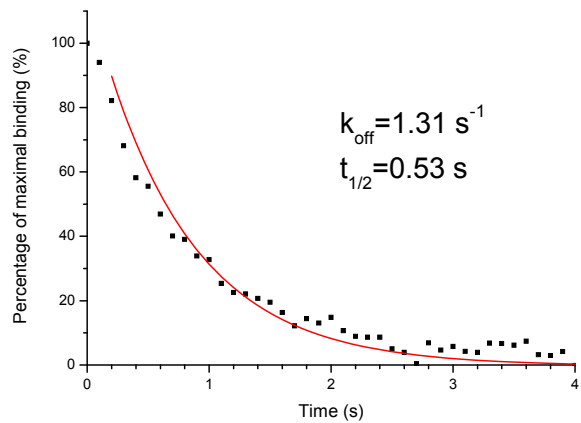
(ii)



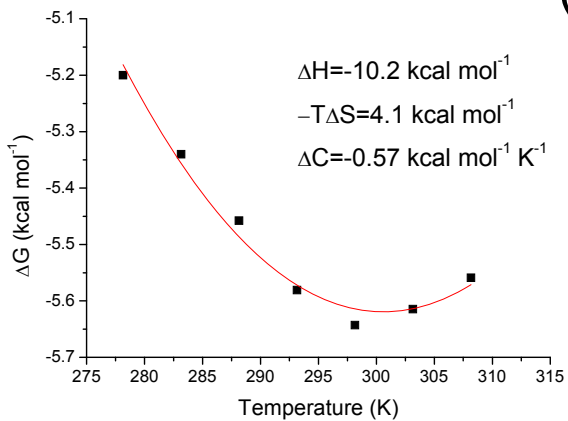
(iii)



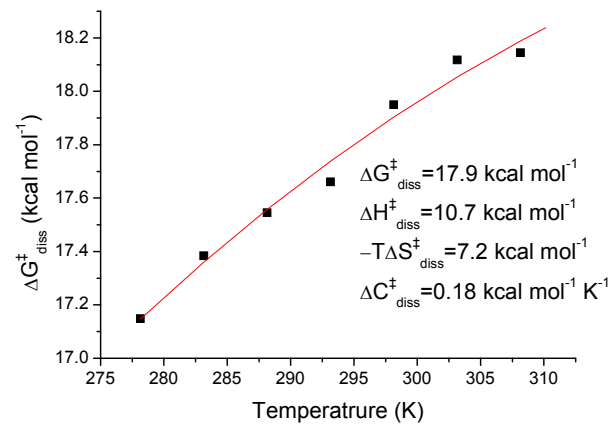
(iv)



(v)

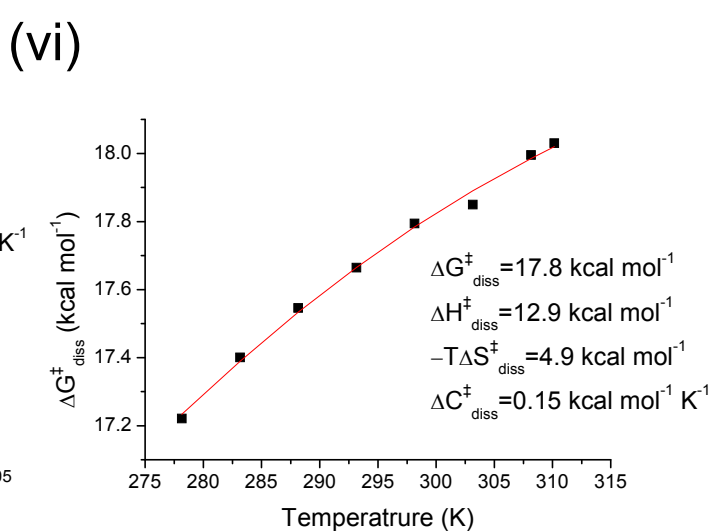
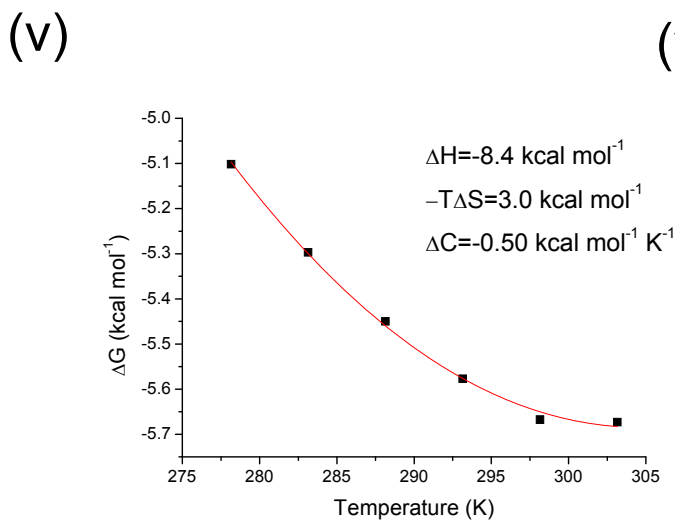
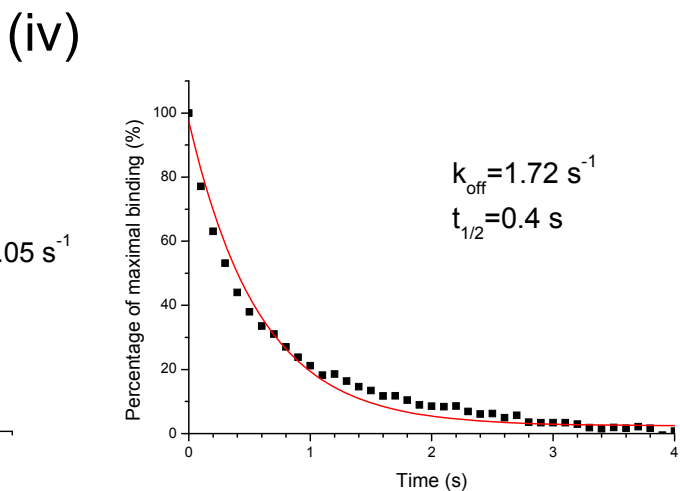
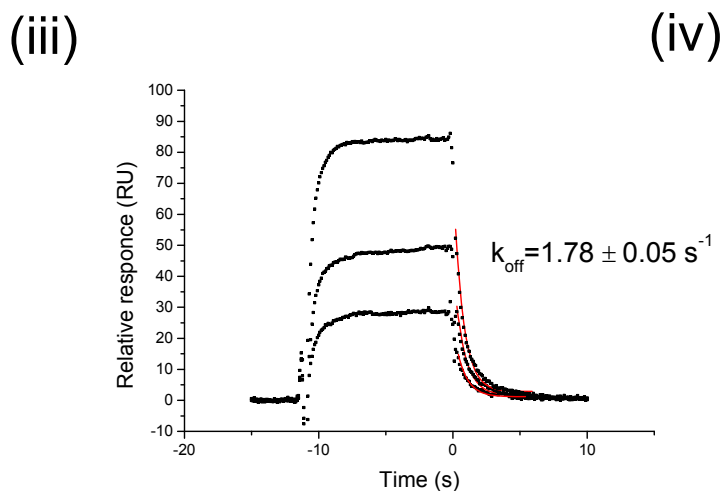
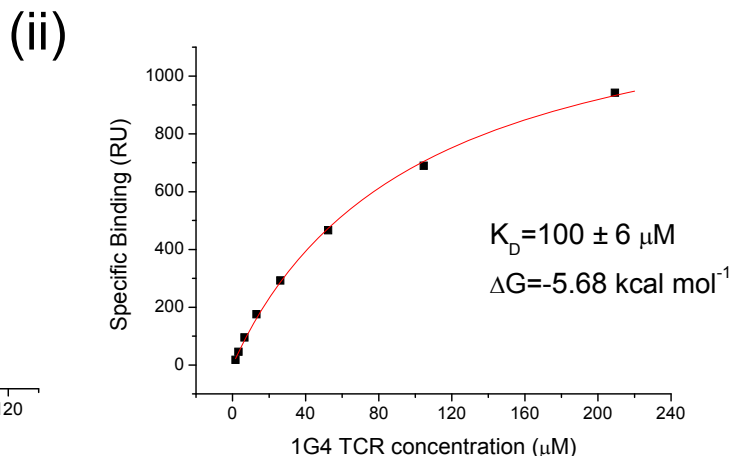
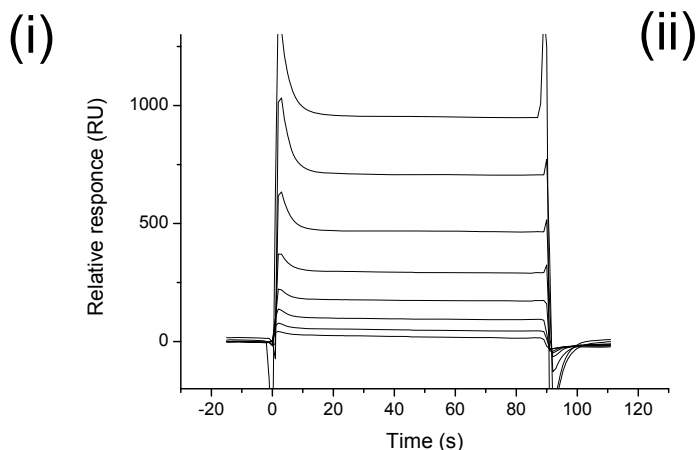


(vi)



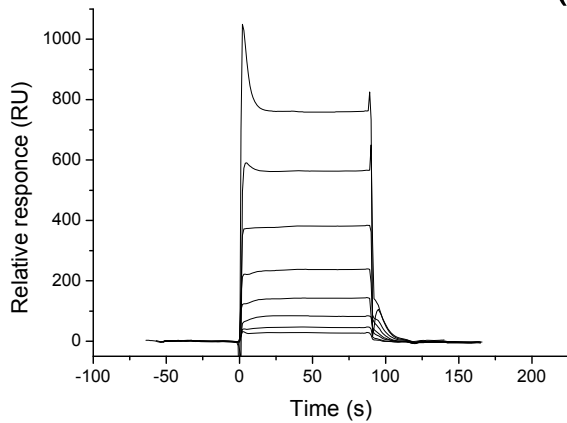


# d) ESO-7H

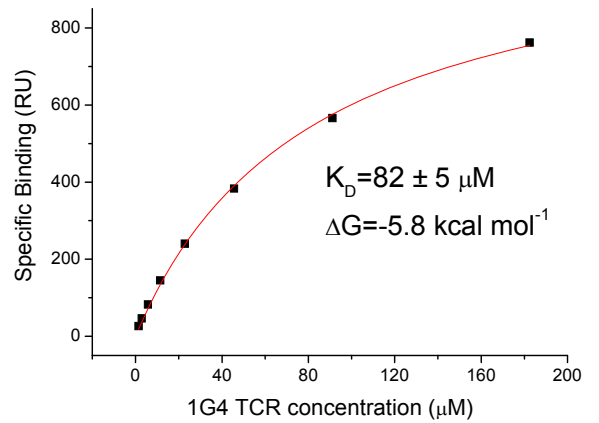


# e) ESO-H70

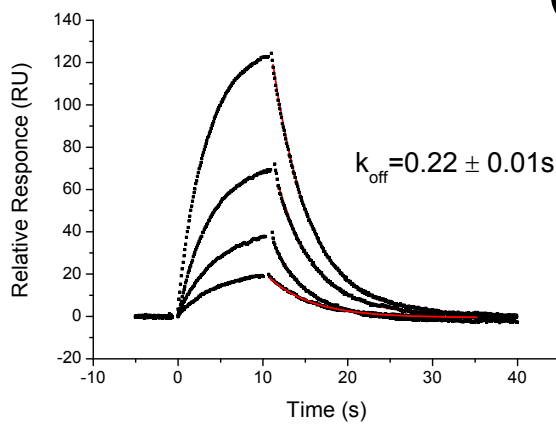
(i)



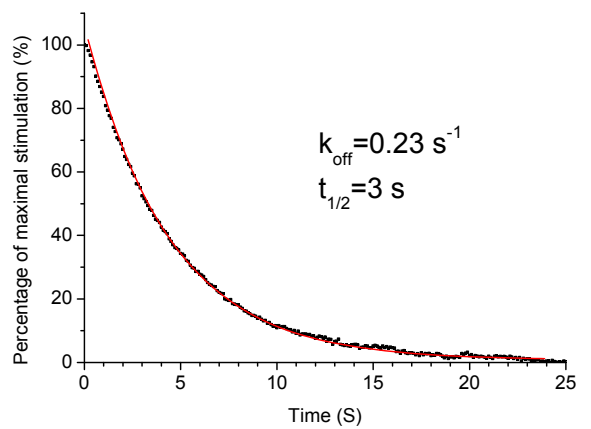
(ii)



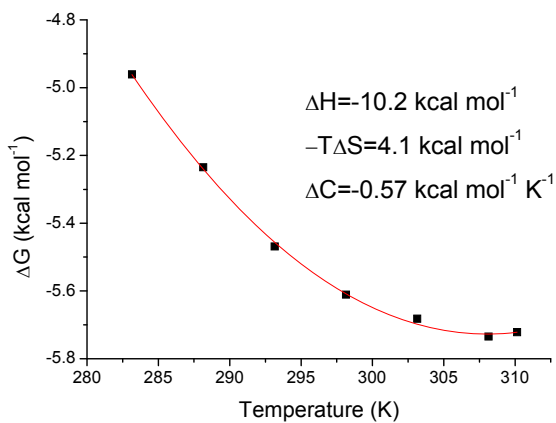
(iii)



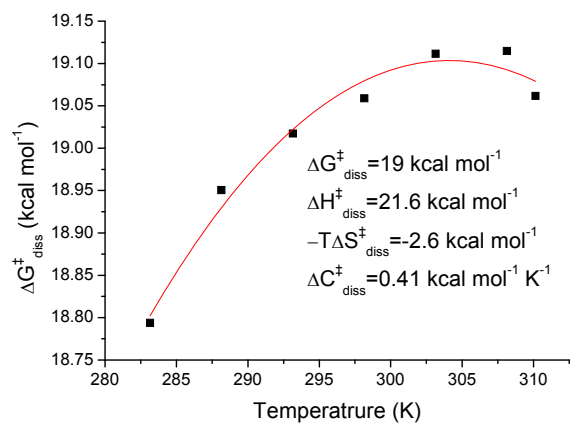
(iv)

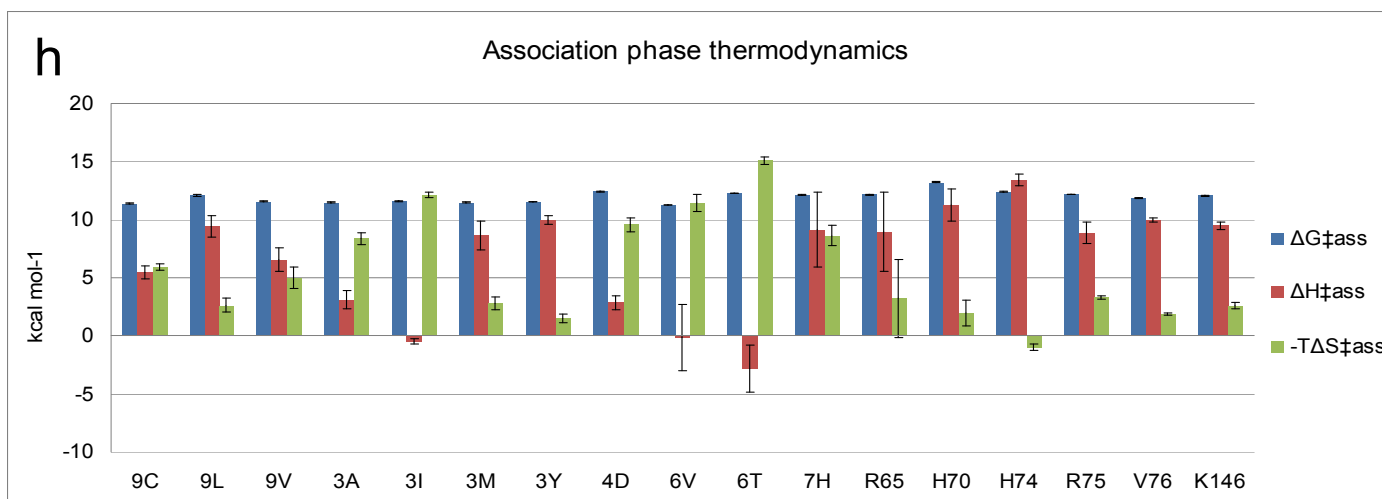
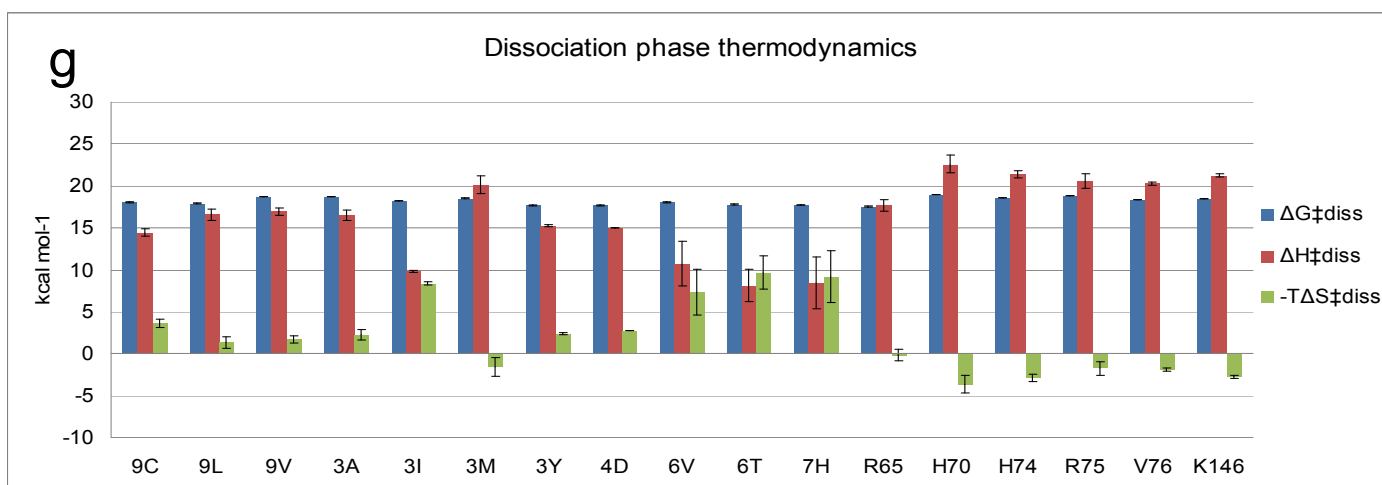
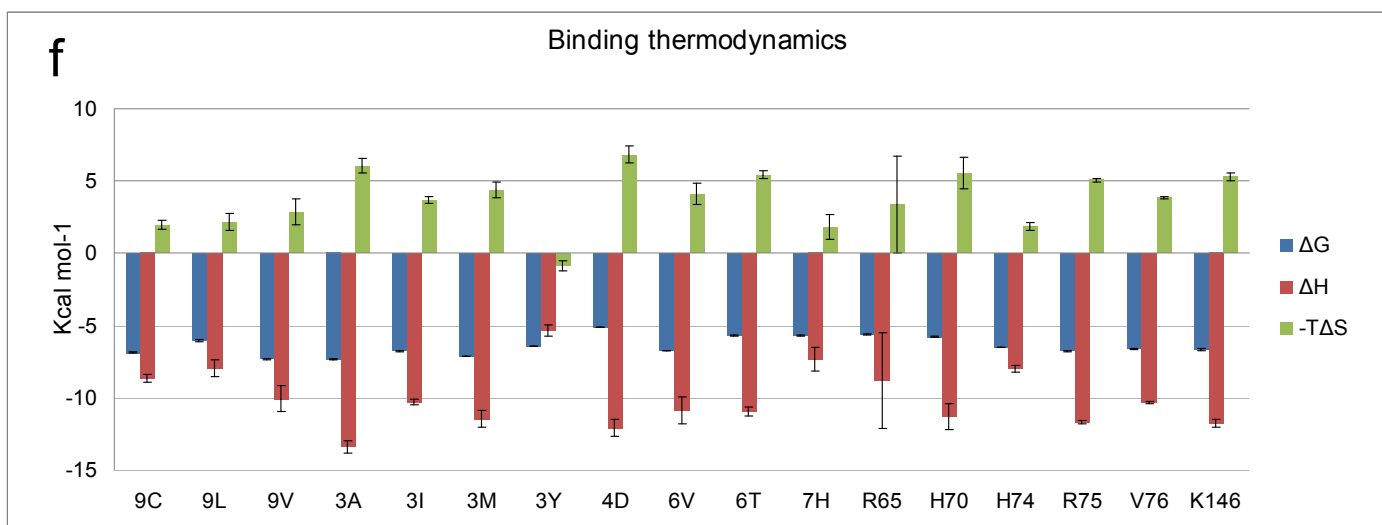


(v)



(vi)





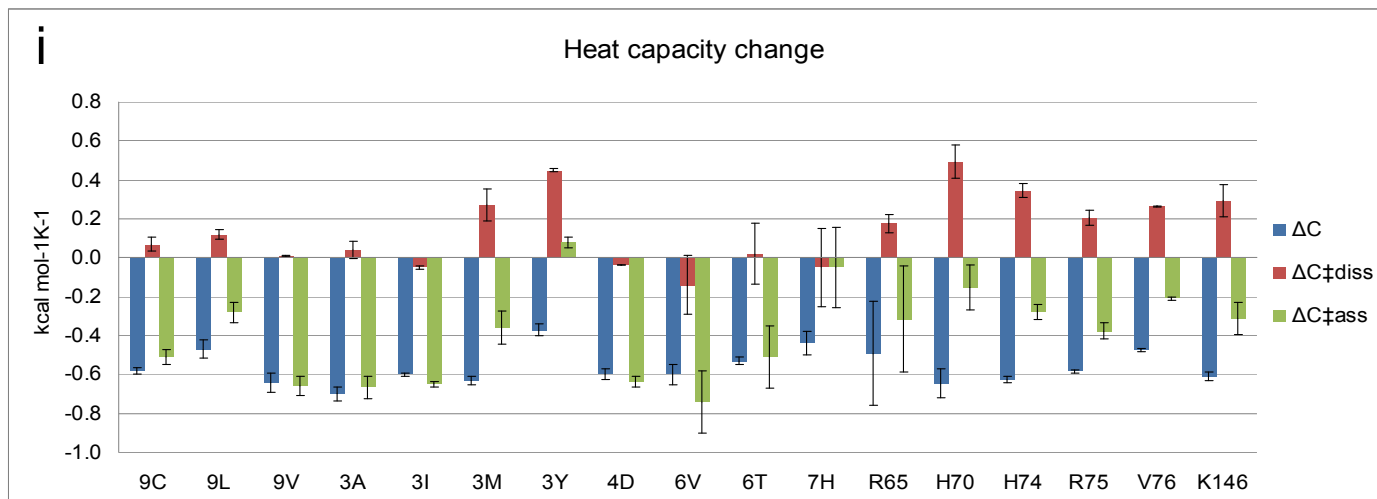


Figure S1: Analysis of 1G4 TCR binding to the ESO-9V pMHC variants.

- a-e) Binding of 1G4 TCR to the ESO-4D (a), A2-R65 (b), ESO-6T (c), ESO-7H (d) and A2-H70 (e) measured by SPR at 37°C
- i) Equilibrium binding of 1G4 TCR (serial two-fold dilutions) to pMHC immobilized to matrix in a biosensor flow cell.
  - ii) Binding at equilibrium (from (i)) plotted against injected TCR concentration. The dissociation constant ( $K_D \pm$  error of fit) was determined by non-linear curve fitting of the equation:  $\text{Bound} = C^A * \text{Max} / (C^A + K_D)$  to the data.  $\Delta G$  was calculated from:  $\Delta G = -RT \ln K_D$  where  $K_D$  is in units M.
  - iii) For kinetic analysis TCR was injected at different concentrations over immobilized pMHC at high flow rates ( $50 \mu\text{L}^{-1} \cdot \text{min}^{-1}$ ) and data collected at 10 Hz. The dissociation rate constant ( $k_{\text{off}}$ ) was determined by fitting the 1:1 Langmuir binding model (red line) to the data (black) using the BIAevaluation program. The  $k_{\text{off}}$  shown is the mean  $\pm$  range ( $n=2$ ) or SD ( $n>2$ ) of the injections shown.
  - iv) Expanded representation of dissociation phase from a single injection in (iii) showing the percentage of the pMHC bound as a function of time.
  - v)  $K_D$  of TCR/pMHC interaction was measured over a range of temperatures from 5°C to 37°C and converted to free energy change ( $\Delta G$ ). Thermodynamic parameters  $\Delta H$ ,  $\Delta S$  and  $\Delta C$  for interaction at 25°C were obtained by fit of the non-linear van't Hoff equation to the data (red line).  $\Delta H$  and  $-T\Delta S$  for interaction at 37°C was calculated from:  $\Delta H_{37^\circ\text{C}} = \Delta H_{25^\circ\text{C}} + 12 * \Delta C_p$  and  $T\Delta S_{37^\circ\text{C}} = T\Delta S_{25^\circ\text{C}} + 310.15^\circ\text{K} * \Delta C_p (\ln(310.15^\circ\text{K}/298.15^\circ\text{K}))$
  - vi)  $k_{\text{off}}$  of TCR/pMHC interaction was measured at the temperatures from 5°C to 37°C and converted to activation energy of dissociation ( $\Delta G_{\text{diss}}^\ddagger$ ). Activation enthalpy, entropy and heat capacity of dissociation ( $\Delta H_{\text{diss}}^\ddagger$ ,  $\Delta S_{\text{diss}}^\ddagger$  and  $\Delta C_{\text{diss}}^\ddagger$ ) were derived from fit of the non-linear van't Hoff equation to the data (red line).
  - f) Comparison of binding thermodynamics of 1G4 TCR interaction with various pMHC variants. Energetic profile of interaction is described by change in binding energy ( $\Delta G$ ), and its enthalpic ( $\Delta H$ ) and entropic ( $-T\Delta S$ ) component.

- f) Comparison of binding thermodynamics of 1G4 TCR interaction with various pMHC variants. Energetic profile of interaction is described by change in binding energy ( $\Delta G$ ), and its enthalpic ( $\Delta H$ ) and entropic ( $-T\Delta S$ ) component
- g-h) Comparison of association and dissociation phase thermodynamics of 1G4 TCR interaction with various pMHC variants
- i) Heat capacity change of association and dissociation phase and total heat capacity change of 1G4 TCR interaction with pMHC variants.

The error bars in f-i represent the SEMs of at least three independent experiments.

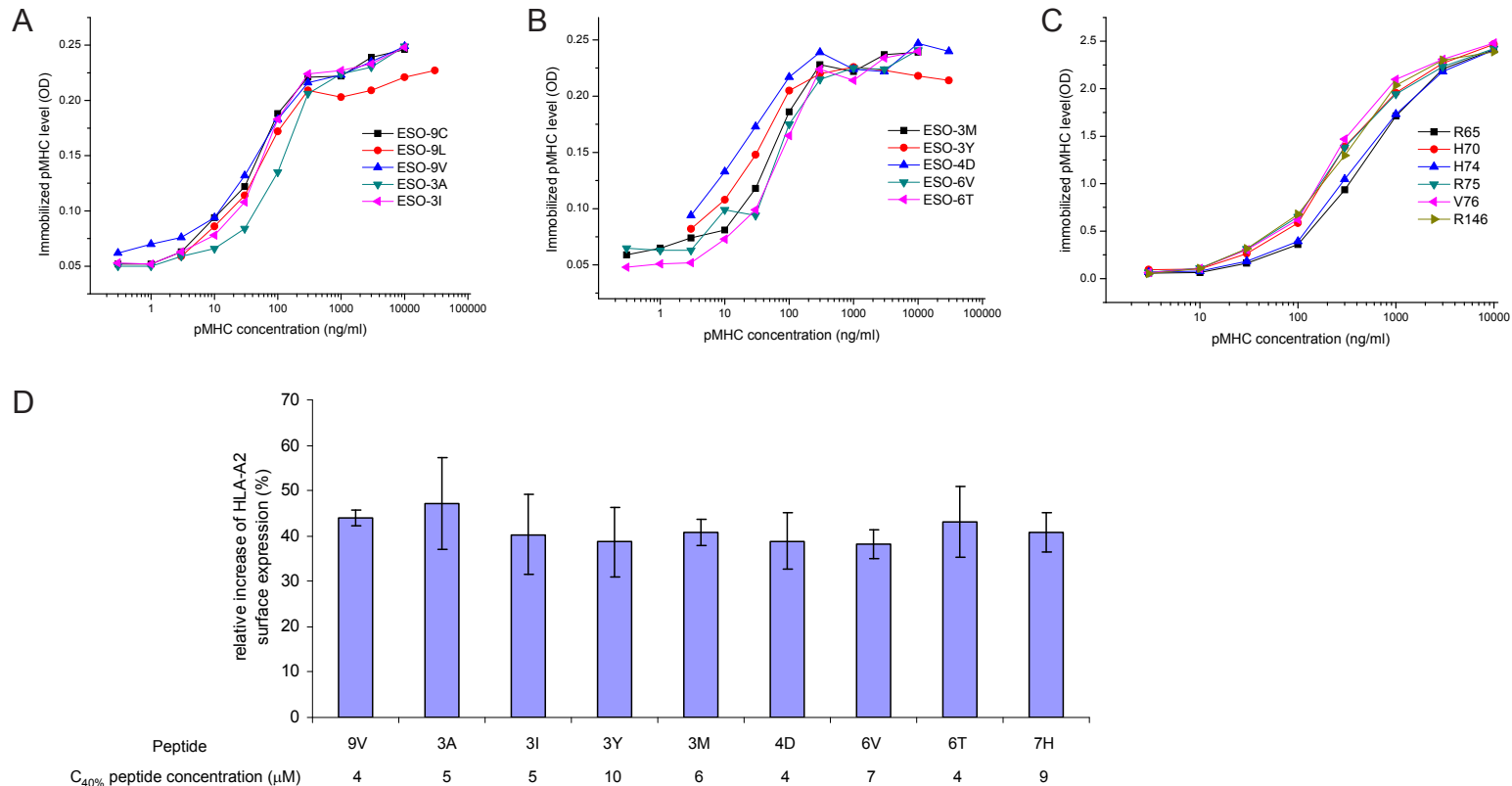


Figure S2: Controlling surface density of pMHC variants in functional assays.

(A-C) After titration of streptavidin-coated 96-well plates with the indicated pMHC variants, the level of immobilized pMHC was measured by ELISA using conformation specific anti-MHC antibody (W6/32).

(D) Confirmation that T2 cells incubated with the indicated concentrations of ESO-9V APLs resulted in comparable 40% increases in surface HLA-A2 expression ( $C_{40\%}$ ) as measured by flow cytometry.

Error bars represent SEMs of at least three independent experiments.

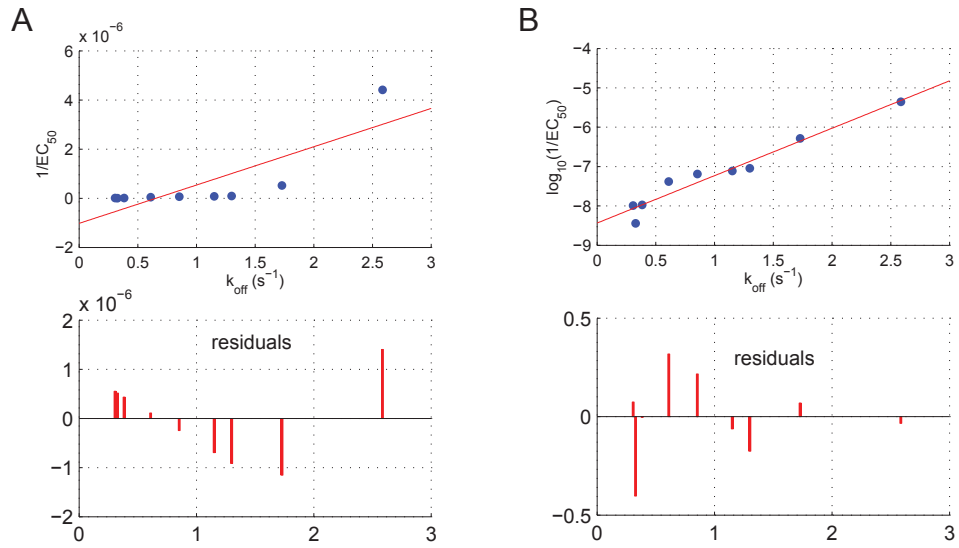


Figure S3: Correlation of T cell response as measured by cytotoxicity assay and  $k_{\text{off}}$ .  
 (a) Direct correlation with  $1/EC_{50}$  shows that residuals are not randomly distributed (lower panel).  
 (b) Taking the log of  $EC_{50}$  improves the correlation and produces random residuals (lower panel).  
 We speculate that there is a non-linear relationship between the concentration of incubated peptide and the level of pMHC presented to T cells by APCs.

pMHC		$K_D$	$K_A$	$k_{off}$	$t_{1/2}$	$k_{on}$	$\Delta G$	$\Delta H$	$-\Delta S$	$\Delta C$	$EC_{50}$ (IFN- $\gamma$ )	$EC_{50}$ (CTL)
peptide name	peptide sequence	( $\mu M$ )	( $mM^{-1}$ )	( $s^{-1}$ )	(s)	$\times 10^3$ ( $M^{-1}s^{-1}$ )	( $kcal\ mol^{-1}$ )	( $kcal\ mol^{-1}$ )	( $kcal\ mol^{-1}$ )	( $kcal\ mol^{-1}K^{-1}$ )	( $\mu g/ml$ pMHC)	$\times 10^5$ ( $C_{40\%}$ dilution)
ESO-9C	SLLMWITQC	14 ± 1	69 ± 3	0.82 ± 0.01	0.84 ± 0.01	57 ± 3	-6.9 ± 0.0	-8.7 ± 0.3	2.0 ± 0.3	-0.58 ± 0.02	115 ± 14	
ESO-9L	SLLMWITQL	56 ± 6	18 ± 2	0.93 ± 0.05	0.74 ± 0.04	17 ± 2	-6.0 ± 0.1	-8.0 ± 0.6	2.2 ± 0.6	-0.47 ± 0.05	426 ± 113	
ESO-9V	SLLMWITQV	7.2 ± 0.5	139 ± 10	0.33 ± 0.01	2.12 ± 0.08	45 ± 4	-7.3 ± 0.0	-10.1 ± 0.9	2.9 ± 0.9	-0.64 ± 0.05	180 ± 19	2777 ± 854
ESO-3A	SLAMWITQV	6.6 ± 0.5	152 ± 12	0.31 ± 0.01	2.26 ± 0.05	47 ± 4	-7.4 ± 0.0	-13.4 ± 0.4	6.1 ± 0.5	-0.70 ± 0.04	70 ± 15	979 ± 330
ESO-3I	SLIMWITQV	17 ± 1	58 ± 3	0.61 ± 0.04	1.14 ± 0.07	35 ± 3	-6.8 ± 0.0	-10.3 ± 0.2	3.7 ± 0.2	-0.60 ± 0.01	94 ± 16	241 ± 91
ESO-3M	SLLMWITQV	9.2 ± 0.2	109 ± 3	0.38 ± 0.01	1.81 ± 0.04	42 ± 1	-7.1 ± 0.0	-11.5 ± 0.6	4.4 ± 0.6	-0.63 ± 0.02	48 ± 7	946 ± 227
ESO-3Y	SLYMWITQV	30 ± 1	33 ± 1	1.15 ± 0.04	0.60 ± 0.02	38 ± 1	-6.4 ± 0.0	-5.3 ± 0.4	-0.85 ± 0.37	-0.37 ± 0.03	240 ± 50	129 ± 26
ESO-4D	SLLDWITQV	252 ± 12	4.0 ± 0.2	2.59 ± 0.15	0.27 ± 0.02	10 ± 1	-5.1 ± 0.0	-12.1 ± 0.6	6.8 ± 0.6	-0.60 ± 0.03	661 ± 85	2.3 ± 0.5
ESO-6V	SLLMWVTQV	18 ± 0	57 ± 1	0.85 ± 0.03	0.81 ± 0.03	49 ± 2	-6.8 ± 0.0	-10.9 ± 0.9	4.1 ± 0.8	-0.60 ± 0.05	45 ± 5	310 ± 85
ESO-6T	SLLMWTTQV	101 ± 5	9.9 ± 0.4	1.30 ± 0.03	0.53 ± 0.01	13 ± 1	-5.7 ± 0.0	-11.0 ± 0.3	5.4 ± 0.3	-0.53 ± 0.02	228 ± 62	111 ± 30
ESO-7H	SLLMWHQV	100 ± 8	10.0 ± 0.8	1.73 ± 0.09	0.40 ± 0.02	17 ± 2	-5.7 ± 0.0	-7.3 ± 0.8	1.8 ± 0.8	-0.44 ± 0.06	526 ± 201	19 ± 6
A2-R65	SLLMWITQV	112 ± 4	8.9 ± 0.3	1.93 ± 0.13	0.36 ± 0.02	17 ± 1	-5.6 ± 0.0	-8.8 ± 3.3	3.4 ± 3.4	-0.49 ± 0.27	479 ± 12	
A2-H70	SLLMWITQV	84 ± 3	12 ± 0	0.22 ± 0.01	3.10 ± 0.09	2.7 ± 0.1	-5.8 ± 0.0	-11.3 ± 0.9	5.6 ± 1.1	-0.65 ± 0.08	151 ± 19	
A2-H74	SLLMWITQV	26 ± 1	39 ± 2	0.49 ± 0.01	1.41 ± 0.02	19 ± 1	-6.5 ± 0.0	-8.0 ± 0.2	1.9 ± 0.3	-0.63 ± 0.02	107 ± 12	
A2-R75	SLLMWITQV	17 ± 1	59 ± 3	0.39 ± 0.00	1.80 ± 0.02	23 ± 1	-6.8 ± 0.0	-11.7 ± 0.1	5.1 ± 0.1	-0.58 ± 0.01	99 ± 12	
A2-V76	SLLMWITQV	22 ± 1	46 ± 2	0.67 ± 0.01	1.04 ± 0.01	31 ± 2	-6.6 ± 0.0	-10.3 ± 0.1	3.8 ± 0.1	-0.47 ± 0.01	146 ± 38	
A2-K146	SLLMWITQV	20 ± 2	50 ± 4	0.48 ± 0.01	1.43 ± 0.02	24 ± 2	-6.7 ± 0.1	-11.8 ± 0.3	5.3 ± 0.3	-0.61 ± 0.02	179 ± 23	

pMHC		$\Delta G^{\ddagger}_{diss}$	$\Delta H^{\ddagger}_{diss}$	$-\Delta S^{\ddagger}_{diss}$	$\Delta C^{\ddagger}_{diss}$	$\Delta G^{\ddagger}_{ass}$	$\Delta H^{\ddagger}_{ass}$	$-\Delta S^{\ddagger}_{ass}$	$\Delta C^{\ddagger}_{ass}$
peptide name	peptide sequence	( $kcal\ mol^{-1}$ )	( $kcal\ mol^{-1}$ )	( $kcal\ mol^{-1}$ )	( $kcal\ mol^{-1}K^{-1}$ )	( $kcal\ mol^{-1}$ )	( $kcal\ mol^{-1}$ )	( $kcal\ mol^{-1}$ )	( $kcal\ mol^{-1}K^{-1}$ )
ESO-9C	SLLMWITQC	18.1 ± 0.0	14.4 ± 0.4	3.6 ± 0.5	0.07 ± 0.04	11.4 ± 0.0	5.5 ± 0.5	5.9 ± 0.3	-0.51 ± 0.04
ESO-9L	SLLMWITQL	17.9 ± 0.0	16.6 ± 0.7	1.3 ± 0.7	0.12 ± 0.02	12.1 ± 0.1	9.4 ± 0.9	2.6 ± 0.6	-0.28 ± 0.05
ESO-9V	SLLMWITQV	18.7 ± 0.0	17.0 ± 0.4	1.8 ± 0.4	0.01 ± 0.00	11.6 ± 0.0	6.6 ± 1.0	5.0 ± 0.9	-0.66 ± 0.05
ESO-3A	SLAMWITQV	18.7 ± 0.0	16.5 ± 0.6	2.2 ± 0.6	0.04 ± 0.04	11.5 ± 0.1	3.1 ± 0.8	8.4 ± 0.5	-0.67 ± 0.06
ESO-3I	SLIMWITQV	18.2 ± 0.0	9.8 ± 0.1	8.4 ± 0.2	-0.05 ± 0.01	11.6 ± 0.0	-0.5 ± 0.2	12.1 ± 0.2	-0.65 ± 0.01
ESO-3M	SLLMWITQV	18.5 ± 0.0	20.1 ± 1.1	-1.6 ± 1.1	0.27 ± 0.08	11.5 ± 0.0	8.7 ± 1.2	2.8 ± 0.6	-0.36 ± 0.09
ESO-3Y	SLYMWITQV	17.7 ± 0.0	15.3 ± 0.1	2.4 ± 0.1	0.45 ± 0.01	11.5 ± 0.0	10.0 ± 0.4	1.5 ± 0.4	0.08 ± 0.03
ESO-4D	SLLDWITQV	17.7 ± 0.0	15.0 ± 0.0	2.7 ± 0.0	-0.04 ± 0.00	12.5 ± 0.0	2.9 ± 0.6	9.6 ± 0.6	-0.64 ± 0.03
ESO-6V	SLLMWVTQV	18.1 ± 0.0	10.7 ± 2.7	7.3 ± 2.8	-0.14 ± 0.15	11.3 ± 0.0	-0.2 ± 2.8	11.4 ± 0.8	-0.74 ± 0.16
ESO-6T	SLLMWTTQV	17.8 ± 0.0	8.1 ± 2.0	9.7 ± 2.0	0.02 ± 0.16	12.3 ± 0.0	-2.8 ± 2.0	15.1 ± 0.3	-0.51 ± 0.16
ESO-7H	SLLMWHQV	17.7 ± 0.0	8.5 ± 3.1	9.2 ± 3.1	-0.05 ± 0.20	35.3 ± 0.1	26.2 ± 3.2	9.0 ± 0.9	0.13 ± 0.21
A2-R65	SLLMWITQV	17.6 ± 0.0	17.7 ± 0.7	-0.17 ± 0.68	0.18 ± 0.05	12.1 ± 0.0	8.9 ± 3.4	3.2 ± 3.4	-0.32 ± 0.27
A2-H70	SLLMWITQV	19.0 ± 0.0	22.6 ± 1.0	-3.6 ± 1.1	0.49 ± 0.09	13.2 ± 0.0	11.3 ± 1.4	1.9 ± 1.1	-0.15 ± 0.11
A2-H74	SLLMWITQV	18.6 ± 0.0	21.4 ± 0.5	-2.9 ± 0.5	0.35 ± 0.04	12.4 ± 0.0	13.4 ± 0.5	-1.0 ± 0.3	-0.28 ± 0.04
A2-R75	SLLMWITQV	18.8 ± 0.0	20.6 ± 0.9	-1.8 ± 0.8	0.21 ± 0.04	12.2 ± 0.0	8.9 ± 0.9	3.3 ± 0.1	-0.38 ± 0.04
A2-V76	SLLMWITQV	18.3 ± 0.0	20.3 ± 0.2	-1.9 ± 0.2	0.26 ± 0.00	11.9 ± 0.0	10.0 ± 0.2	1.9 ± 0.1	-0.21 ± 0.01
A2-K146	SLLMWITQV	18.5 ± 0.0	21.3 ± 0.2	-2.7 ± 0.2	0.30 ± 0.01	12.0 ± 0.1	9.5 ± 0.3	2.6 ± 0.3	-0.31 ± 0.03

Table S1: Biophysical and functional characterisation of 1G4 TCR interaction with pMHC variants. Binding affinity, kinetics and thermodynamics of 1G4 TCR to various peptide and MHC mutants were measured at 37°C by SPR (Figure S1). Activation potency of each pMHC in IFN $\gamma$  release assay and cytotoxicity assay is presented by  $EC_{50}$  value. Mean values of at least three independently performed experiments are shown  $\pm$  standard error of mean (SEM).



pMHCs removed	$K_D$		$k_{off}$		CM			MF			CM + MF			
	$b_0 + b_1 * K_D$		$b_0 + b_1 * k_{off}$		$b_0 + b_1 * k_{off} / (k_{on} + b_2)$			$b_0 + b_1 * k_{off} * \exp(b_2 * C_p)$			$b_0 + b_1 * k_{off} * \exp(b_3 * C_p) / (k_{on} + b_2)$			
	$b_0$	$b_1$	$b_0$	$b_1$	$b_0$	$b_1$	$b_2$	$b_0$	$b_1$	$b_2$	$b_0$	$b_1$	$b_2$	$b_3$
0	92	2.49	2.5	247	41.84	11.22	0.034	5.4	375	0.81	65.3	29	0.003	3.91
1	72	3.09	8.3	238	37.04	9.13	0.022	40.9	712	2.51	79.7	78	0.001	6.35
2	79	2.79	11.4	233	33.94	9.51	0.022	52.7	812	2.98	84.8	107	0.000	7.29
3	99	1.74	58.3	147	62.19	6.06	0.016	82.8	721	3.58	87.1	98	0.000	7.19
4	87	2.37	50.4	163	-10.59	10.26	0.009	84.3	751	3.72	34.4	23	0.004	2.49
5	82	2.29	51.2	162	-10.35	10.22	0.009	89.1	262088	14.67	78.2	680	0.000	10.14
6	85	2.37	45.0	167	-13.14	10.22	0.009	79.5	786	3.77	33.9	27	0.004	2.91
7	89	2.25	56.5	166	-5.10	10.72	0.010	91.1	273132	14.77	80.3	711	0.000	10.25
8	105	2.06	68.7	163	-0.22	10.04	0.010	101.4	623	3.37	47.1	25	0.004	2.71
9	95	2.31	57.5	163	-1.96	10.47	0.010	87.0	711	3.55	34.9	22	0.005	2.28

Table S2. Fitted parameter values for each data subset considered in Table 2 in main text.